MODELING AND EXPERIMENTAL STUDY OF SHORT PERIOD CHANGES IN GALACTIC COSMIC RAYS INTENSITY*

M.V. Alania

Institute of Mathematics and Physics, University of Podlasie
3 Maja 54, 08-110 Siedlce, Poland
and
Institute of Geophysics, Georgian Academy of Sciences, Tbilisi, Georgia

A. Barczak and A. Wawrzyńczak

Institute of Computer Science, University of Podlasie
Sienkiewicza 51, 08-110 Siedlce, Poland

(Received March 11, 2003)

We study short period changes in galactic cosmic rays (GCR) intensity and analyze features of its sporadic and recurrent decreases (Forbush effects). We show that the energy spectrum of Forbush effect is suitable for investigating the structure of irregularities of the interplanetary magnetic field, resulting from shock waves and magnetic clouds in the interplanetary space. This study is based on experimental data from neutron monitors and on theoretical modeling of GCR transport.

PACS numbers: 96.40.–z

1. Introduction

A fast decrease in GCR intensity during a period of one to two days and then its gradual recovery in 4–6 days is called the Forbush effect [1]. This effect is generally related to the shock waves and magnetic clouds in the interplanetary space formed after the outstanding flares on the Sun [2]. Phenomena of this kind appear by chance, sporadically, without any regularities. At the same time there exist the recurrent Forbush effects associated with the disturbances repeating with the period of the rotation of the Sun. The recurrent Forbush effects have approximately symmetric time-profile with

* Presented at the XV Marian Smoluchowski Symposium on Statistical Physics, Zakopane, Poland, September 7–12, 2002.

respect to the minimum intensity of GCR. Usually, an intensity of GCR decreases for the period of 5–7 days and recovers approximately during the same time period. The Forbush effects are related to the active regions on the Sun living for a few solar rotations. The problem of resolving of the recurrent Forbush effects and the 27-day variation of the GCR intensity has not been solved [3].

Fig. 1 shows changes in the GCR intensity during the sporadic Forbush effect of March 9–23, 1989. Fig. 2 shows the recurrent Forbush effect of September 1–16, 1996. It can be seen that the amplitude of the sporadic Forbush effect is much larger than that of the recurrent one. However, this

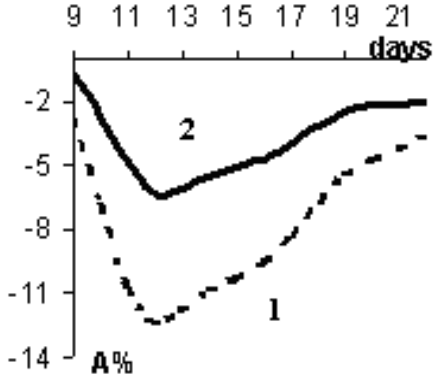

Fig. 1. Forbush effect of the GCR intensity by Kiel (1) and Tokyo (2) super monitor data for the period of March 9–23, 1989.

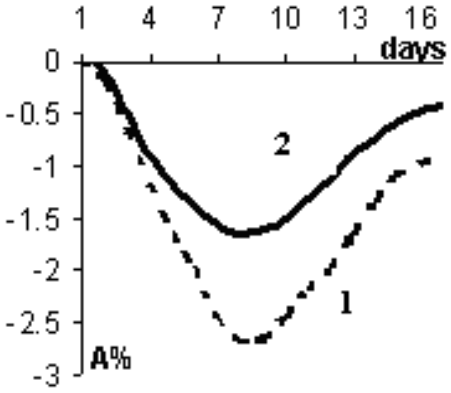

Fig. 2. Forbush effect of the GCR intensity by Goose Bay (1) and Roma (2) super monitor data for the period of September 1–16, 1996.

is not always the case. In general, the average amplitudes of the recurrent Forbush effect are less than that of the sporadic one. The sporadic Forbush effects are produced by powerful and dynamically developing disturbances in the interplanetary space, while the recurrent Forbush effects are connected with relatively weak and well established co-rotating disturbances.

2. Energy spectrum of the Forbush effect

One of the most important parameters characterizing the Forbush effect is the rigidity spectrum of the GCR intensity variations, $\delta D(R)/D(R) = AR^{-\gamma}$, where R is the rigidity of GCR particles and A is the power of the rigidity spectrum of Forbush effect. The rigidity spectrum shows a dependence of the amplitude of the GCR intensity decrease on the rigidity of the particles. So, the power A is equal to the amplitude of Forbush effect for the GCR particles of 1 GV rigidity. The energy spectra of the Forbush effects presented on figures 1, 2 have been calculated using the data from neutron super monitors. According to [4,5], we have assumed that

$$\begin{aligned} \frac{\delta D(R)}{D(R)} &= AR^{-\gamma} \quad \text{for } R \leqslant R_{\max}\,, \\ \frac{\delta D(R)}{D(R)} &= 0 \qquad \text{for } R > R_{\max}\,, \end{aligned} \tag{1}$$

where $R_{\max}$ is the upper limiting rigidity beyond which the Forbush effect vanishes. The amplitude of the relative changes of the GCR isotropic intensity variation $\delta J_i/J_i$ (secondary neutron component intensity variation of GCR) at any point of observation with the geomagnetic cut off rigidity R_i and the average atmospheric depth h_i is defined as

$$\frac{\delta J_i}{J_i} = \int\limits_{R_i}^{R_{\max}} \frac{\delta D(R)}{D(R)} W_i(R, h_i)\, dR\,, \tag{2}$$

where the weight function $W_i(R, h_i)$ is the coupling coefficient of GCR [4]. Coupling coefficients for each of the neutron monitors in forms suitable for calculating the energy spectrum of GCR variations have been presented by a Japanese group [5]. For the power energy spectrum of the type (1), Eq. (2) can be written as

$$\frac{\delta J_i}{J_i} = A_i \int\limits_{R_i}^{R_{\max}} R^{-\gamma} W_i(R, h_i)\, dR\,, \tag{3}$$

from which we get

$$A_i = \frac{\delta J_i}{J_i} \left[\int_{R_i}^{R_{\max}} R^{-\gamma} W_i(R, h_i)\, dR \right]^{-1} . \tag{4}$$

A_i is the variation of the primary GCR intensity in the interplanetary space and theoretically should be the same for all neutron monitors. In practice, for various reasons (*e.g.* different statistics of the experimental data, some uncertainties in the correction of the barometric effects and so on), A_i slightly differ from each other. As data for a number of neutron monitors are available, we have minimized $\sum_i (A_i - A)^2$ (where A is the average of A_i) with respect to γ and $R_{\max}$. The accuracy of the calculated value of γ is not better than 5–10% in spite of the high accuracy of ($\geqslant$0.05%) daily averaged neutron monitors data used. This results from a limited accuracy of coupling coefficients for different neutron super monitors in various epochs of solar activity. Admitting changes in $R_{\max}$ has little effect; an acceptable value of $R_{\max}$ is about (150–200) GV. This stems from the fact that the coupling coefficients for neutron monitors $W_i(R, h_i)$ rapidly tend to zero for rigidities larger than that.

3. Experimental results and their interpretation

The 14 neutron monitors with different cut off geomagnetic rigidities used for calculating the energy spectrum of the Forbush effects of March 9–23, 1989 and September 1–16, 1996 are identified in Table I. Results of these calculations are presented in figures 3 and 4.

It can be seen from figure 3 that the energy spectrum of the Forbush effect is soft at the periods of decreasing of GCR intensity and hard when the GCR intensity recovers. This kind of variations is connected to the specific changes of the structure of the nearby interplanetary space where Forbush effect of GCR of March 9–23, 1989 has occurred.

Specifically, at the beginning of the GCR intensity decrease the disturbances in the interplanetary space develop and undergo a spatial extension. The velocity of disturbances (shock waves or magnetic clouds) is large and an intensive convection of GCR takes place. Due to both of these reasons, low energy particles of GCR are preferentially modulated and γ is large (γ = 1.3–1.5) and the energy spectrum of the Forbush effect is soft. Then the size of the disturbances increases (the vicinity of the shock waves and magnetic clouds is extended) and due to the interaction of these relatively high velocity disturbances with the background solar wind, new irregularities with larger sizes are created [6]. Due to these reasons, higher energy

TABLE I

Neutron monitors used for calculating the energy spectrum of the March 9–23, 1989 event. Stations marked by an asterisk * are used also for the calculating the energy spectrum of the September 1–16, 1996 event.

Station	Cut off rigidity [GV]	Station	Cut off rigidity [GV]
Apatity	0.68	Kiev	3.62
Beijing	9.56	Lomnicki Stit	4.00
Calgary*	1.09	Moscow*	2.46
Goose Bay*	0.52	Oulu*	0.81
Hyancayo	13.45	Potchefs	7.30
Irkutsk	3.66	Rome*	6.32
Kiel*	2.29	Tokyo	11.61

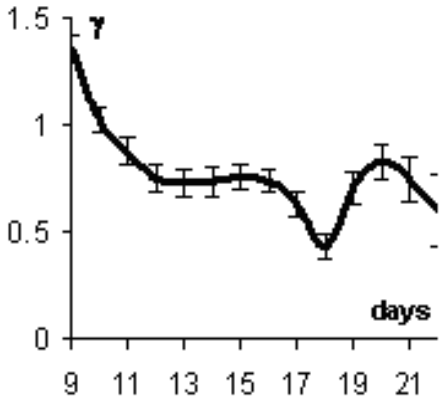

Fig. 3. Temporal changes of the energy spectrum exponent γ of the sporadic Forbush effect of March 9–23, 1989.

particles are preferentially modulated and result in the hard energy spectrum of the Forbush effects that is, in fact, observed ($\gamma = 0.5$–0.6) in the experimental data from neutron monitors (Fig. 3).

This explanation applies to these GCR modulations in which the diffusion-convection approximation is valid. This scenario takes place for many cases of the sporadic Forbush effects when the disturbances occupy a large size of the inner heliosphere and a geometrical factor of these disturbances does not play any important role. However, that is not always so. Sporadic

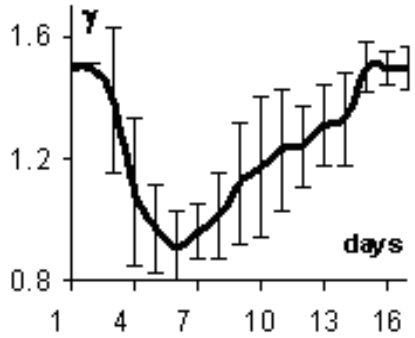

Fig. 4. Temporal changes of the energy spectrum exponent γ of the recurrent Forbush effect of September 1–16, 1996.

Forbush effects with peculiar properties related directly to the geometrical factor and specific structure of the shock waves, magnetic clouds and intensity of the coronal mass ejecta, have been observed [2,7,8].

Temporal changes of the rigidity exponent of the recurrent Forbush effect of September 1–16, 1996 are presented in figure 4. It should be stressed that when the amplitudes of the Forbush effects are small ($\leqslant 2\%$), the accuracy of the calculated γ smaller than when the amplitudes of Forbush effect are large. Unfortunately, for the recurrent Forbush effect this problem is frequently present. It can be seen in figure 4 that at the beginning of the gradual decrease of the GCR intensity, the energy spectrum is soft ($\gamma = 1.4$–1.5), near the minimum intensity of GCR the energy spectrum becomes relatively hard ($\gamma = 0.9$–1.0), and during the gradual recovery the energy spectrum becomes soft again ($\gamma = 1.4$–1.5). During the recurrent Forbush effect dynamical processes in the interplanetary space and the temporal changes of the rigidity spectrum exponent γ of GCR intensity variations have features that are rather different than those presented in the figure 3 for the sporadic Forbush effect. In particular, the Earth slowly enters the Co-rotating region of the disturbances and low energy particles of GCR are strongly modulated. This leads to the soft energy spectrum of GCR. Then the Earth continues its voyage to the depths of the extended disturbances where GCR particles with higher energies are modulated and the energy spectrum of Forbush effect hardens. Later the Earth slowly leaves this region and the contribution from the high energy particles of GCR gradually diminishes, leading to the soft energy spectrum. This kind of changes of the energy spectrum of the recurrent Forbush effect of GCR is the standard one related to the geometrical size of the disturbances in the interplanetary space. Changes of GCR intensity for the period of September 1–16, 1996 correspond to the this type of the Forbush effect.

4. Discussion

As it was shown by Alania and Iskra [7], the diffusion–convection approximation of the isotropic intensity variations of GCR (11 years variations) leads to the rigidity exponent γ related to a parameter α connecting the diffusion coefficient K and the rigidity R of GCR ($K \propto R^{\alpha}$) and thus can be used to analyze the structure of IMF's irregularities. The same can predicted when the diffusion–convection approximation is applied to the Forbush effect. If it is the case, the temporal (daily) changes of the energy spectrum exponent provide the means for making statements about the electromagnetic properties, and the structural evolution of the IMF's irregularities of that part of the interplanetary space that is occupied by the disturbances (vicinity of the extended shock waves, magnetic clouds and *etc.*), in particular. This is an inverse problem of the GCR modulation. For the diffusion–convection scenario, the rigidity spectrum of the Forbush effect can be used as a source of information on the disturbed interplanetary medium. Bearing in mind that there is not enough experimental data on the IMF's irregularities for any reliable spectral analysis (due to short times of the disturbances in the interplanetary space), data on GCR intensity become very even more valuable. Indeed, the parameter α showing the dependence of the diffusion coefficient K on the rigidity R of GCR particles depends on the IMF's structure [9] and varies between zero and two. The minimum value of $\alpha = 0$ can be associated with the type of scattering that occurs when the Larmor radius ρ of GCR particles is slightly less or comparable to the effective size L of the IMF's irregularities ($\rho \leqslant L$) and the scattering angle φ is large. This is the case when a scattering free path λ and, correspondingly, the diffusion coefficient K of cosmic ray particles do not depend on the particle's rigidity R. On the other hand, the maximum value of $\alpha = 2$ can be associated with scattering of cosmic ray particles on the IMF's irregularities when the Larmor radius ρ of the GCR particles of the given energy is larger than that the effective size L of the magnetic irregularities of the IMF ($L < \rho$). In this case the scattering angle φ of GCR particles on the individual irregularities is small, i.e. $\varphi \leqslant 5°$–$10°$, and the scattering free path λ and the diffusion coefficient K strongly depend on the particle's rigidity R, $K \propto \lambda \propto R^2$. It has been found that the energy spectrum exponent γ of the GCR isotropic intensity variations depends on the parameter α, ($\gamma \propto \alpha$) [7]. The parameter α characterizes the structure of the IMF's irregularities (turbulence) being responsible for the GCR particle's scattering [9, 10]. As the energy spectrum exponent γ of the GCR isotropic intensity variations depends on α, there must be an explicit relationship between γ and the parameters characterizing the structure of the irregularities of the IMF. In the minimum level of intensity, when the energy spectrum of

the Forbush effect is hard, the irregularities of the IMF responsible for the scattering of the GCR particles must display greater average effective sizes than at the beginning of the Forbush effect. The additional larger irregularities of the IMF can be created as a result of interactions between the relatively high velocity disturbances and the background solar wind. It has been shown [9, 10] that $\alpha = 2 - \nu$, where ν is the exponent of the power spectrum density (PSD) of the IMF's irregularities (PSD$\propto f^{-\nu}$, where f is the frequency). Therefore, in case of a direct relationship between γ and α, one can write $\gamma \propto 2 - \nu$. According to the experimental results presented in figures 3 and 4, it can be concluded that the parameter ν, the exponent of the power spectrum density (PSD) of the IMF's irregularities, varies in the ranges $0.6 < \nu < 1.5$ for the sporadic Forbush effect and $0.5 < \nu < 1.1$ for the recurrent Forbush effect. Thus, analysis of the temporal changes in the energy spectrum exponent, γ, provides prospective means of studying the structure of IMF irregularities during the Forbush effects.

5. Modeling the recurrent Forbush effect

We have used Parker transport equation [11] to model the Forbush effect:

$$\frac{\partial N}{\partial t} = \nabla_i \left(K_{ij} \nabla_j N \right) - \nabla_i \left(U_i N \right) + \frac{1}{3R^2} \frac{\partial \left(R^3 N \right)}{\partial R} \left(\nabla_i U_i \right), \tag{5}$$

where N and R are, respectively, the density (in the interplanetary space) and the rigidity of GCR particles. The first term on the right hand side of Eq. (5) describes diffusion due to the symmetric part and drift due to the antisymmetric part of the anisotropic diffusion tensor K_{ij}. The second term describes convection and the third term the change of the energy (acceleration/cooling) of GCR particles due to the interactions with solar wind. U_i is the solar wind velocity and t is the time. Due to small changes in the GCR intensity during the recurrent Forbush effect (the intensity changes by 2–3% in the period of 5–7 days), the $\partial N/\partial t$ term can be neglected. At the same time, the assumed changes of the solar wind velocity and the diffusion coefficient, together with the limited range of the heliolongitudes lead to a decrease in the GCR intensity similar to the recurrent type of the Forbush effect. Indeed, moving in the azimuthal direction and crossing the Co-rotating disturbances, one can observed the Forbush effect. Eq. (5) in the spherical coordinates reads

$$\begin{aligned} A_1 \frac{\partial^2 n}{\partial r^2} \quad & + A_2 \frac{\partial^2 n}{\partial \theta^2} + A_3 \frac{\partial^2 n}{\partial \varphi^2} + A_4 \frac{\partial^2 n}{\partial r \partial \theta} + A_5 \frac{\partial^2 n}{\partial r \partial \varphi} + A_6 \frac{\partial^2 n}{\partial \theta \partial \varphi} \\ & + A_7 \frac{\partial n}{\partial r} + A_8 \frac{\partial n}{\partial \theta} + A_9 \frac{\partial n}{\partial \varphi} + A_{10} \frac{\partial n}{\partial R} + A_{11} n = 0 . \end{aligned} \tag{6}$$

In this equation, n is the relative density, $n = N/N_0$, where N_0 is density of GCR in the interstellar medium with $N_0 \propto R^{-4.5}$ for this range of rigidities to which neutron monitors are sensitive. The dimensionless distance $r = \rho/r_0$, where r_0 is the size of the modulation region and ρ is the distance from the Sun. A_1, A_2, ..., A_{11} are functions of r, θ, φ and R. Eq. (6) has been solved for two cases: $\delta = 0^\circ$ and $\delta = 20^\circ$, viz. for the two- and three-dimensional IMF.

The anisotropic diffusion tensor is an important parameter for the modulation of GCR. Due to the fact that the structure of the IMF is obscure, this tensor has many uncertainties. In the spherical coordinates $B(B_r, B_\theta, B_\varphi)$ this tensor reads [12, 13]

$$K_{11} = K_{\parallel}\left[\cos^2\delta\cos^2\psi + \beta\left(\cos^2\delta\sin^2\psi + \sin^2\delta\right)\right], \tag{7a}$$

$$K_{12} = K_{\parallel}\left[\sin\delta\cos\delta\cos^2\psi\,(1-\beta) - \beta_1\sin\psi\right], \tag{7b}$$

$$K_{13} = K_{\parallel}\left[\sin\psi\cos\delta\cos\psi\,(\beta-1) - \beta_1\sin\delta\cos\psi\right], \tag{7c}$$

$$K_{21} = K_{\parallel}\left[\sin\delta\cos\delta\cos^2\psi\,(1-\beta) + \beta_1\sin\psi\right], \tag{7d}$$

$$K_{22} = K_{\parallel}\left[\sin^2\delta\cos^2\psi + \beta\left(\sin^2\delta\sin^2\psi + \cos^2\delta\right)\right], \tag{7e}$$

$$K_{23} = K_{\parallel}\left[\sin\delta\sin\psi\cos\psi\,(\beta-1) + \beta_1\cos\delta\cos\psi\right], \tag{7f}$$

$$K_{31} = K_{\parallel}\left[\cos\delta\sin\psi\cos\psi\,(\beta-1) + \beta_1\sin\delta\cos\psi\right], \tag{7g}$$

$$K_{32} = K_{\parallel}\left[\sin\delta\sin\psi\cos\psi\,(\beta-1) - \beta_1\cos\delta\cos\psi\right], \tag{7h}$$

$$K_{33} = K_{\parallel}\left[\sin^2\psi + \beta\cos^2\psi\right], \tag{7i}$$

where δ is the angle between the lines of the IMF and the radial direction in the meridian plane ($\delta = \arctan(B_\theta/B_r)$. ψ is the angle between the lines of the IMF and radial direction from the Sun ($\psi = \arctan(-B_\varphi/B_r)$). β and β_1 are the ratios of the perpendicular $K_\perp$ and drift K_d diffusion coefficients to parallel $K_\parallel$ diffusion coefficient with respect to the regular IMF lines ($\beta = K_\perp/K_\parallel$ and $\beta_1 = K_d/K_\parallel$), respectively.

The existence of three-dimensional IMF's has been proposed in Refs. [14–16]. In order to compare the roles of each component of the tensor for a three dimensional IMF, all components of this tensor for different values of δ have been calculated. Results of calculations for $\delta = 0^\circ$ and $\delta = 20^\circ$ are presented in figure 5. The ordinate axes of the all panels show normalized magnitudes of K_{11}, K_{12}, ..., K_{33}. One can see that there are significant differences for some components of the tensor between the two- and three-dimensional cases.

Parameters included in Eq. (5) and determined during the course of the recurrent Forbush effect have the following expressions: The parallel diffusion coefficient, $K_\parallel$, is represented as $K_\parallel = K_0 K(r)K(\theta,\varphi)K(R)$, where $K(\theta,\varphi) = 1 - 0.5\sin(3(\varphi - 75^\circ))\sin^6(\theta)$, $K(R) = (R/1\mathrm{GV})^\alpha$, $K(r) =$

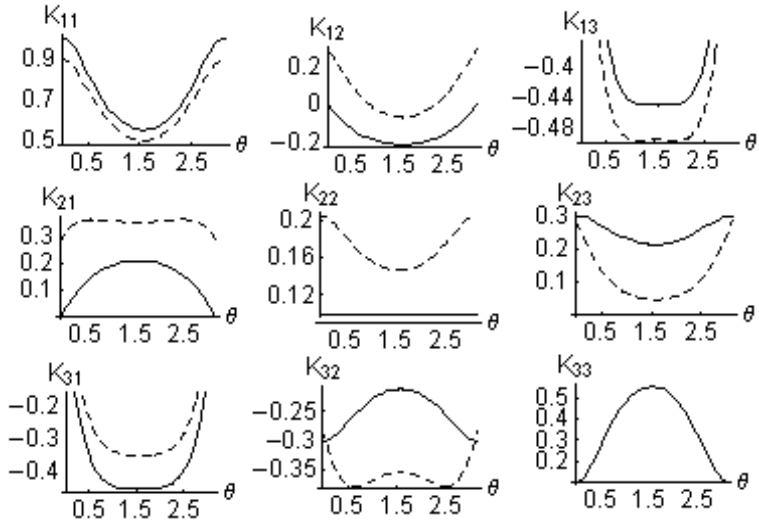

Fig. 5. Changes in the anisotropic diffusion tensor for two- (solid line) and three- (dashed line) dimensional IMF *versus* heliolatitudes.

$1.+0.5(r/1\mathrm{AU})$. Here r is the dimensionless distance from the Sun in the astronomical units (AU) and R is the rigidity in GV. The product $K_0K(R)$ is equal to $2\times10^{22}\,\mathrm{cm^2s^{-1}}$ at the rigidity of $R=10\,\mathrm{GV}$ for $\alpha=1$ and remains constant for an arbitrary α in the range $0<\alpha<1.2$. The solar wind velocity is $U=U_0(1+0.5\sin(3(\varphi-75^\circ))\sin^6(\theta))$. $\beta=0.1$ at the Earth's orbit for the rigidity $R=10\,\mathrm{GV}$ of GCR particles and then it changes *versus* the spatial coordinates according to the Parker's spiral magnetic field. The size of the modulation region is equal to 100 AU and the background solar wind velocity $U_0=400\,\mathrm{km/s}$. The disturbances causing the Forbush effect are confined within $\pm30^\circ$ of the heliolatitudes with respect to the helioequator ($60^\circ\leqslant\theta\leqslant120^\circ$) and within $75\leqslant\varphi\leqslant135^\circ$ of the heliolongitudes. To avoid the intersections of the IMF's lines due to the changes in the solar wind velocity, the disturbances are confined in the radial direction up to 7–8 AU. Eq. (6) has been solved numerically using the finite difference method. This equation does not contain time but is of the parabolic type with respect to the rigidity R of GCR particles. Therefore, Eq. (6) is similar to the heat conducting equation and has a form of an ordinary Cauchy problem for the partial differential equation. The following initial and boundary conditions have been used:

$$\left.\frac{\partial n}{\partial r}\right|_{r=0}=0\,,\quad n|_{r=1}=1\,,\quad n|_{\theta=0}=n|_{\theta=180^\circ}\,,\quad n|_{R=150\mathrm{GV}}=1\,,$$
$$n|_{\varphi=0}=n|_{\varphi=360^\circ}\,. \tag{8}$$

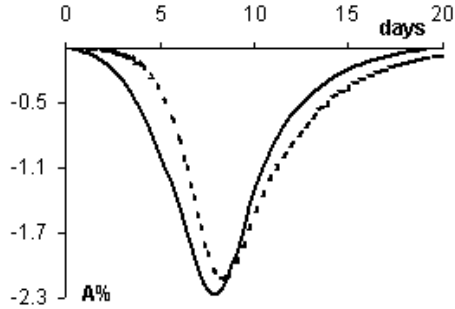

Fig. 6. The recurrent Forbush effect at the energy of 10 GV for the two- (solid line) and three- (dashed line) dimensional IMF *versus* heliolongitudes.

The solutions of Eq. (6) are presented in figure 6. Solid curve corresponds to the $\delta = 0^\circ$ (two dimensional IMF) and dashed curve to the $\delta = 20^\circ$ (three dimensional IMF) cases, respectively. It can be seen from this figure that the simulated Forbush effect corresponds to the recurrent Forbush effect observed experimentally (figure 2). In both these cases symmetric gradual decreases and recoveries of the intensity of GCR lasting for similar periods of time ($\sim$ 7 days) are observed. The amplitude of the expected Forbush effect is greater for the two dimensional than that for the three dimensional IMF. This effect must be related to the decrease in the diffusion coefficients for the two dimensional IMF.

6. Conclusions

1. Temporal changes of the energy spectrum exponent γ of the sporadic and recurrent Forbush effects of GCR reflect changes in the large scale structure of the IMF's irregularities in this part of the interplanetary space where shock waves, magnetic clouds and other types of turbulences dominate in the course of Forbush effects.

2. Temporal changes of γ corresponding to the sporadic and the recurrent Forbush effects differ: In powerful sporadic Forbush effects significant hardening of the energy spectrum during the decreasing phase of the GCR intensity are observed. The hard spectrum remains almost constant or softens only slightly during the recovery phase of GCR intensity. These changes of the energy spectrum are related to additional, large-size irregularities of IMF created as a result of interactions between high velocity particles and the background solar wind. In the recurrent Forbush effects the spatial structure of irregularities of the IMF is stationary and the decisive role belongs to the geometrical factor: to the sizes of the disturbances. When the Earth

enters the co-rotating region of the disturbances, the low energy particles of GCR are preferentially modulated, leading to the soft energy spectrum of Forbush effect. Then the Earth continues its voyage to the depths of the extended disturbances where GCR particles with higher energies are modulated and the energy spectrum of Forbush effect hardens. Then the Earth slowly leaves this region and the energy spectrum of Forbush effect again becomes soft.

3. Temporal changes in γ provide means of determining the structure of the irregularities during the course of the sporadic and recurrent Forbush effects of GCR.

REFERENCES

[1] S.E. Forbush, *J. Geophys. Res.* **59**, 525 (1954).

[2] H.V. Cane, *Space Sci. Rev.* **93**, 49 (2000).

[3] M.V. Alania, D.G. Baranov, M.I. Tyasto *et al.*, *Adv. Space Res.* **27**, 619 (2001).

[4] L.I. Dorman, *Cosmic Rays Variations and Space Explorations*, Elsvievier, New York 1974.

[5] S. Yasue, S. Mori, S. Sakakibara, K. Nagashima, Coupling Coefficients of Cosmic Ray Daily Variation for Neutrons Monitor Stations, Nagoya 1982.

[6] M.V. Alania *et al.*, 8th ECRC, A.3.7, Rome (1982).

[7] M.V. Alania, K. Iskra, *Adv. Space Res.* **16**, 241 (1995).

[8] N.A. Nachkebia, M.A. Despotashvili, E.O. Fluckiger, Proc. 27th ICRC, Hamburg, 9, 3548 (2001).

[9] I.N. Toptygin, *Cosmic Rays in the Interplanetary Magnetic Field*, Reidel Holland, 1985.

[10] J.R. Jokipii, *Rev. Geophys. Space Phys.* **9**, 1 (1971).

[11] E.N. Parker, *Astrophys. J.* **128**, 664 (1958).

[12] M.V. Alania, Modulation of Cosmic Rays, Proceedings of the Institute of Geophys. Georgian Academy of Sciences, Tbilisi, 1978, page 5 (in Russian).

[13] V.M. Alania, Variation of Cosmic Rays, Georgian Academy of Science, Mecniereba, Tbilisi, 1980, page 11 (in Russian).

[14] K. Nagashima, K. Munkata, R. Tatsuoka, *Planet Space Sci.* **34**, 1299 (1986).

[15] J. Jokipii, J. Kóta, *Geophys. Res. Lett.* **16**, 1 (1989).

[16] L.A. Fisk, *J. Geophys. Res.* **101**, 15547 (1996).